Theoretical modelling of steps on the CaF$_2$(111) surface

V E Puchin[1]**, A V Puchina**[1]**, M Huisinga**[1] **and M Reichling**[2,3]

[1] Fachbereich Physik, Freie Universität Berlin, Arnimallee 14, 14195 Berlin, Germany
[2] Department Chemie, Universität München, Butenandtstraße 5–13, 81377 München, Germany

E-mail: reichling@cup.uni-muenchen.de

Abstract
The atomic and electronic structure and relaxation of the perfect (111) surface
and several low-index surfaces of CaF$_2$ are calculated using an *ab initio* Hartree–
Fock method. We find marked differences between the bulk and surface valence
band structures; however, the band gap is reduced by only 0.5 eV for the stepped
surface. The (111) surface is found to exhibit no significant relaxation and we
obtain a surface energy of 0.47 J m^{-2}. The atomic structure of two types
of stepped surface both having 0.32 nm high steps aligned along the [110]
crystallographic direction is determined and the step energies are found to be
0.25 and 0.35 nJ m^{-1}, respectively. Step energies for configurations involving
other orientations of steps are considerably higher. The formation of double-
height steps along [110], however, is found to be energetically favourable. A
considerable amount of relaxation is found for stepped surfaces and we explain
qualitatively why it results in a roughening of the surface in some cases. The
energetic position of gap electronic states induced by steps on the (111) surface
is found to be very similar to that for surface states of the perfect (111) surface;
i.e. such states do not yield a significant density of states more than 0.5 eV above
the bulk valence band maximum. We discuss how the step formation energies
found here might explain surface topographical features found on cleaved and
grown CaF$_2$(111) surfaces.

1. Introduction

Laser ablation and the resistivity of optical materials against laser pulses with sub-band-gap
photon energy strongly depend on the purity of the crystal and the quality of its surface. Surface
defects and adsorbed species induce local electronic states in the insulator band gap, initiating
optical absorption. The absorbed energy is transferred to the lattice and may cause damage and
ablation, especially when dealing with high-power laser light [1]. Information about the atomic
and electronic structure of particular surface defects can be very helpful for achieving a detailed

---

[3] Author to whom any correspondence should be addressed.

understanding of the basic mechanisms of such laser degradation processes. Absorbing defects in the band gap are most relevant in the ultraviolet (UV) spectral region since, due to the high energy of UV photons, defects may induce linear absorption even in wide-band-gap materials. Among these, CaF_2 is one of the most notable ones, since it is a stable, chemically rather inert material that can be grown as a single crystal of high quality and combines a wide band gap of close to 12 eV with convenient optical properties [2]. Advanced polishing techniques allow surface processing of CaF_2 to highest optical quality [3] and, therefore, this material is a promising candidate for use in high-performance optical lens systems [4] for the next generation of UV laser steppers operated a wavelength of 193 nm [5]. Such lens systems involve a large number of surfaces and, therefore, it is an important task to understand the structural and optical properties of such surfaces.

Steps are unavoidably present at any cleaved crystalline surface. Recent scanning force microscopy studies of $CaF_2(111)$ surfaces shows that cleavage creates a large number of steps with heights ranging from 0.32 nm corresponding to one F–Ca–F triple layer to macroscopic size. A typical distance between triple-layer steps is 10 nm, but the distance varies strongly with cleavage conditions. The predominant features of the surface topography are either cleavage tips with a tip angle of typically 45° or extremely sharp features with only a few-degree tip angle [6, 7]. However, having a statistics of hundreds of such experiments, we find that tip angles larger than 90° never occur by cleavage. The results presented here provide some possible explanations for the observed predominance of small tip angles.

When an intense laser beam hits a step, damage may occur at intensities much lower than the damage threshold of a flat (111) terrace [8]. However, it is not yet clear whether this is caused by enhanced light absorption due to electronic properties of the step, by extrinsic effects like defect accumulation at the step, by optical effects like electric field enhancement at the step, by a reduction of the fracture strength in the vicinity of the step, or by a combination of such effects.

A comparative study of $CaF_2(111)$ surfaces cleaved in air and in ultrahigh vacuum probing the density of occupied electronic states in the band gap by ultraviolet photoelectron spectroscopy reveals that there is a tail of emission extending from the valence band about 6 eV into the band gap for air-cleaved crystals, while there is no measurable band-gap emission for vacuum-cleaved crystals [9]. This result indicates that cleavage steps do not introduce band-gap states, and one important reason for performing the present work is to confirm this from a theoretical point of view.

The electronic structure of the perfect $CaF_2(111)$ surface has previously been calculated using the semi-empirical LCAO method [10]; however, surface relaxation effects were neglected. Earlier calculations of the surface structure and dynamics including relaxation were performed in the framework of the shell model [11, 12]. Both calculations predicted the reduction of the distance between the topmost fluorine and next calcium layers. However, the magnitude of this relaxation depends on the parameters of the pair potential model. It varies between 19% [11] and 1.7% [12] of the interlayer distance.

The structure of the $CaF_2(110)$ surface and its melting have been studied using classical molecular dynamics simulation and both rigid-ion and shell models for pair interaction potentials [13]. It was found that the missing-row reconstruction, giving alternate (111) and (11$\bar{1}$) micro-facets along the [001] direction, is energetically favourable.

The electronic structure of $CaF_2(111)$ with a completely removed topmost fluorine layer, as an example of a defective surface, was calculated and for this configuration an additional half-filled band was found in the middle of the band gap [14]. Band-gap states were also found in molecular cluster calculations of the electronic structure of the $CaF_2(111)$ with surface F centres and F-centre clusters [15].

The purpose of the present paper is to develop an atomistic model for cleavage steps on the CaF$_2$(111) surface and to study the modifications in the surface density of states induced by steps. The main question to be answered is whether, in the presence of steps, occupied or empty states are created in the band gap of the perfect crystal and to what extent surface electronic bands are distorted. Furthermore, we aim to achieve a better understanding of the topography of cleaved and fractured surfaces. With our methods, we cannot directly simulate the cleavage process involving complicated dynamics and local energies much higher than static surface energies. However, we analyse different surface geometries and discuss their stability in terms of the total energy to provide a qualitative understanding of the predominance or absence of specific configurations found in experiments.

2. Method of calculation

All calculations presented here were performed using an *ab initio* Hartree–Fock method and a slab model as implemented in the CRYSTAL95 computer code [16]. We employed the Gaussian basis sets 8-6-5-11G* for Ca^{2+} and 7-311G F$^-$ ions that have been optimized for the bulk CaF$_2$ crystal by Catti *et al* [17]. They found that the basis-set extension with a polarization d orbital at the Ca^{2+} ion leads to a lattice parameter contraction by 1.1%. Therefore, some of our calculations have been performed with an additional set of 3G-contracted d functions at Ca^{2+} ions [17]. Other computational parameters controlling the accuracy of the calculation, such as truncation criteria for electronic integrals, and dimensions of the integration net in the reciprocal space, have been chosen good enough to ensure that the error in the total energy was less than 10^{-5} Hartree.

The surface energy γ_{ijk}, i.e. an energy per unit area, was calculated as the difference between the total energy per unit cell E_s of the slab parallel to the (ijk) crystallographic plane and the normalized energy E_b of the bulk related to the surface area σ_{uc} of the unit cell:

$$\gamma_{ijk} = (E_s - mE_b)/2\sigma_{uc}. \tag{1}$$

The bulk energy E_b is multiplied by the number of CaF$_2$ molecules in the slab unit cell m, because the elementary unit cell of the bulk crystal contains only one CaF$_2$ molecule while there might be several of them in the slab unit cell depending on the slab thickness. The factor of two is introduced to account for the fact that a slab has two surfaces.

Next, we aimed to establish structural and energetic properties of surface steps. An *ab initio* calculation of single steps having periodicity only in one dimension could in principle be performed using CRYSTAL95; however, we expected such calculations to be rather demanding as regards computing time, due to the large number of ions in the unit cell needed for a correct step simulation. Therefore, we chose the more convenient route of performing calculations on a regular array of steps, such as are present on vicinal cut surfaces.

The step formation energy ε_{st} was determined as the difference between the surface energy of the stepped surface γ_{ijk} and that of the flat (111) surface. To obtain an energy independent of the specific plane investigated, this energy was related to the number of steps present and the difference in slab unit-cell areas was taken into account:

$$\varepsilon_{st} = (\gamma_{ijk} - \gamma_{111}\cos\alpha)d/\sin\alpha. \tag{2}$$

Here d denotes the step height and α is the angle between the (ijk) and (111) planes.

In order to obtain the equilibrium structure of the slabs, the total energy was calculated at a sufficient number of points around the expected minimum in the atomic configuration space. The adiabatic potential energy surface was then approximated with a quadratic form using a least-squares fit to the calculated points. The geometry of the slabs was optimized over a

complete set of independent internal coordinates, taking into account symmetry constraints. Each of the slabs considered had at least two symmetry elements: inversion and a mirror plane perpendicular to the slab. Translation vectors parallel to the slab were kept constant throughout the geometry optimization. The value of 0.5538 nm as predicted by Hartree–Fock calculations for the bulk crystal [17] was used for the lattice parameter. The dependence of the results on the slab thickness was studied for the (111), (110), and (100) surfaces.

To obtain a density of states (DOS) that can be compared to experimental data, the calculated projected DOS was convoluted with a Gaussian function. The width at half-maximum of this function was chosen to be 1 eV, which is a typical value for phonon broadening observed in UPS of wide-band-gap insulators [18].

3. The ideal (111) surface

A CaF_2 crystal has the fluorite structure and is composed of F–Ca–F triple layers in the (111) direction. These are the natural cleavage planes of the crystal [19]. The structure of this (111) plane and that of some other low-index planes relevant in the context of the present work are shown schematically in side view (bottom figure) in figure 1. The perfect (111) cleavage plane is F^- terminated and the topmost F^- ions form a hexagonal array. The threefold symmetry of the surface is determined by the Ca^{2+} and F^- ions in the second and third planes, as seen in the top view (top figure) of figure 1.
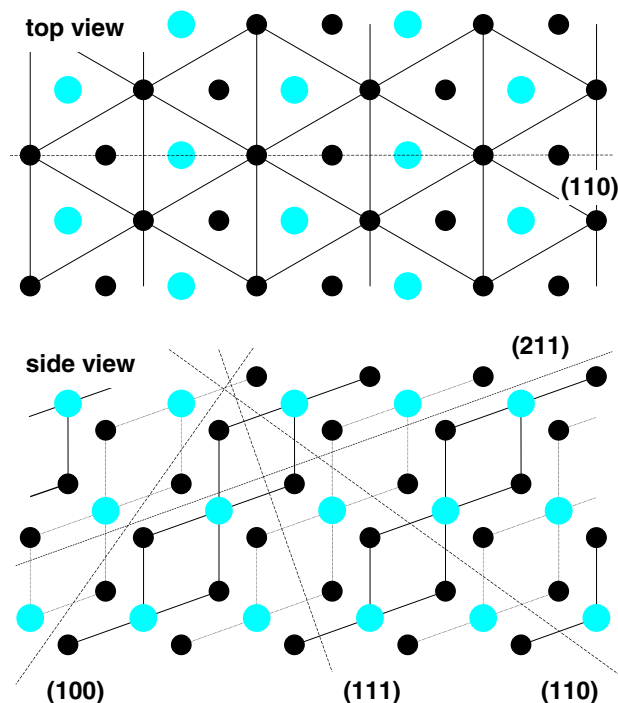

Figure 1. The structure of the $CaF_2(111)$ surface in top view and side view. Black circles denote positions of F^- ions while larger grey circles indicate Ca^{2+} ions. Solid lines connect ions situated in the plane of the diagram. Dotted lines connect ions which are in the next parallel (110) plane. Dashed lines show intersections of the plane of the diagram with some low-index planes.

Surface energies for slabs of increasing thickness are listed in table 1. The distances between the layers in the slabs were optimized and we found that the atomic relaxation is negligible. The calculated displacements of the atoms are less than 0.01 Å and thus the (111) surface is an ideal termination of the bulk structure. This result strongly differs from earlier calculations by Jockisch *et al* [11], where a considerable relaxation was found, and is in better agreement with Tasker's work [12]. The surface energy was found to be 0.47 J m^{-2} in good agreement with experimental data [20] and an earlier calculation based on the pair inter-ionic potentials and the shell model [12, 13].

Table 1. Surface energy, relaxation, and rumpling for CaF$_2$(111), CaF$_2$(110), and CaF$_2$(100). Convergence of results with slab thickness.

Surface	Number of atomic layers in the slab	Approximate slab thickness (pm)	Surface energy (J m^{-2})		Relaxation (pm)	Rumpling (pm)
			Non-relaxed	Relaxed		
(111)	3	160	0.487	0.484	1.5	—
	6	480	0.471	0.466	−1.0	
	9	800	0.471	0.467	−0.7	
	12	1120	0.471	0.467	−0.2	
(110)	2	200	0.930	0.769	−7.5	22.5
	3	390	0.939	0.856	−2.5	9.5
	4	590	0.939	0.817	−4.7	15.3
	5	780	0.939	0.826	−3.6	13.0
	6	980	0.939	0.819	−4.2	13.6
	7	1170	0.939	0.819	−4.9	13.1
(100)	3	280	1.419	0.925	41.0	—
	5	550	1.506	1.120	31.1	
	7	830	1.508	1.181	28.4	
	9	1110	1.508	1.189	26.4	
	11	1380	1.508	1.189	27.1	

The charges of ions in the surface layers are almost the same as in the bulk or in deeper layers of the slab. We found a charge of −0.97 for the top-layer F$^-$ and +1.94 for the second-layer Ca^{2+}, whereas the bulk charges are −0.99 and +1.98, respectively, reflecting the high degree of ionic bonding in this crystal. The energy of the highest occupied state of the valence band lies −15 eV below the vacuum level; the one-electron energies of the shallow core levels are −34, −40, and −59 eV for Ca (3p), F (2s), and Ca (3s) levels, respectively. According to Koopmans' theorem, these values provide an upper estimate for the electron binding energies. The same order of levels has been suggested for the interpretation of photoelectron spectroscopy data [21]. Our theoretical values are higher by about 8 eV due to neglecting electron correlation and hole relaxation.

The surface band gap and the width of the F (2p) valence band found in the slab calculations for the perfect (111) surface are almost the same as those for in the bulk, if the phonon broadening is not taken into account. There are no surface states higher in the band gap. However, the density of states projected to the surface F$^-$ ion differs significantly from that of the bulk. In figure 2 the projected DOS for the first five F$^-$ layers is compared to that of the bulk. In contrast to the bulk DOS, having two peaks of almost equal height, the DOS of the topmost layer (F$_1$) has only one peak with a maximum close to the top of the valence band. To compare the bulk DOS with the surface DOS, the difference in Madelung potential
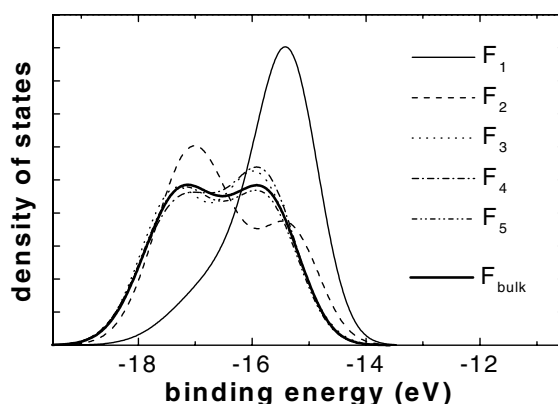
Figure 2. The projected density of states in the F (2p) valence band for different F^- ions in a 15-layer $CaF_2(111)$ slab. The labels F_i denote fluorine layers, starting from the surface with F_1. The solid bold line represents the bulk density of states.

between the infinite crystal and the slab has to be taken into account. For the representation in figure 2 we shifted the bulk DOS in energy so that it matches the DOS of the deepest layer in the slab which has electronic properties very close to those of the bulk. The p_x, p_y, and p_z components of the surface DOS are almost equal to each other. For the deeper layers F_2 to F_5, the DOS rapidly approaches the bulk structure. The different shape of the surface-projected DOS and its shift towards lower electron binding energy with respect to the bulk DOS yields the effective broadening of the F (2p) valence band and reduces the surface band gap.

The electronic states of the (111) surface and its structural relaxation were calculated with an sp basis set as well as with additional polarization d functions for Ca^{2+}. We found, however, that the d functions have very little effect on the equilibrium geometry, surface energy, and electron density of states. Therefore, further calculations of other low-index surfaces have been performed with the sp basis set only, to save computation time, which is important because the symmetry of the other surfaces is lower than that of the (111) surface.

4. (110) and (100) surfaces

The CaF_2 crystal cannot be cleaved along low-index surfaces other than (111). Therefore, we expect (110) and (100) surfaces to have higher surface energies. Atomic layers on the (110) surface contain one Ca^{2+} and two F^- ions per unit cell that is neutral. In contrast, the (100) slab consists of alternating F^- and Ca^{2+} layers with a charge of ± 2 per unit cell. In this case, surface reconstruction is most likely to maintain a zero surface dipole moment. We have chosen to remove half of the F^- ions from the terminating F^- layers, halving the charge of the top surface layer. This modification reduces the surface symmetry but does not extend the unit cell. Table 1 shows the dependence of the calculated surface energies on the slab thickness. Surface relaxation as listed in table 1 is defined as a decrease of the distance between the first and second surface layers with respect to the bulk crystal. In the case of the (110) surface, the displacements of F^- ions in the top surface layer are positive (outwards) while the Ca^{2+} undergo negative displacements. The distance between Ca^{2+} and F^- sub-layers is the measure of rumpling shown in table 1. In this case the mean distance between the first two layers is used to calculate the relaxation. Our results for the (110) surface are in qualitative agreement with shell-model calculations. Lindan [13] reports a 12% decrease in spacing between the two

outermost Ca^{2+} planes to be compared with 8% found in the present calculations. In earlier work by Tasker [12], the (110) surface rumpling was found to be 7.6% of the interlayer spacing and yield a relaxation of 5.4%, while our calculations yield 6.7% and 2.5% for rumpling and relaxation, respectively.

We find that the convergence of energy with slab thickness is better for non-relaxed surfaces and that the relaxation energy is larger for the less stable surfaces. In the worst case of the (100) surface, a slab of about 0.8 nm thickness is required to achieve a precision of 0.01 J m^{-2}. We expect surfaces having a smaller angle with the (111) cleavage plane to have lower surface energies and to exhibit better convergence with the slab thickness in terms of surface energy and structure.

5. Steps on the (111) surface

The structure of the (111) surface shown in figure 1 is the only one found to be stable for stoichiometric CaF$_2$. A surface terminated by Ca or another F layer would have a non-zero dipole moment, leading to surface instability. Therefore, the minimum height of any step on CaF$_2$(111) is equal to 0.32 nm representing one F–Ca–F triple layer.

The most symmetric steps on the (111) surface having the simplest structure are those with their edges aligned along close-packed F rows in [110] directions (solid lines in the top view of figure 1). Three equivalent orientations of such elementary steps are possible due to the threefold surface symmetry. For each orientation there are two types of step differing in their direction of descent. To model steps of various structures in a periodic way suitable for our calculations, we consider vicinal cuts through the crystal along a series of planes listed in table 2. The two types of descent yield two sequences of stepped surfaces (S_n^{I} and

Table 2. Three sequences of low-index CaF$_2$ surfaces with different types of step. All sequences converge to the (111) surface in the limit of infinite n. The angle between the surface and this basic (111) plane is decreasing with n, while the distance between steps or the width of (111) terraces is increasing. Surfaces marked with asterisks are in fact flat, but they can be considered as stepped surfaces with an extremely high density of steps.

	n	S_n	Angle with base (111) (deg)	Distance between steps (pm)
Type I	−1	(111)	70.53	111*
($n+2, n+2, n$)	0	(110)	35.26	446*
	1	(331)	22.00	780
	2	(221)	15.79	1115
	3	(553)	12.27	1449
	4	(332)	10.68	1783
Type II	0	(100)	54.74	223*
($n+2, n, n$)	1	(311)	29.50	557
	2	(211)	19.47	892
	3	(533)	14.42	1226
	4	(322)	11.42	1560
Type III	0	(210)	39.23	386
($n+4, n+2, n$)	1	(531)	28.56	579
	2	(321)	22.21	772
	3	(753)	18.09	965
	4	(432)	15.23	1158

S_n^{II}, $n = 0, 1, 2, \ldots, \infty$) converging to (111) at infinite n. For both sequences, the distance between steps increases with n and the angle with respect to the (111) base plane decreases. For small n, the distance between steps is comparable to or even smaller than the step height and the resulting surfaces are atomically flat. However, they can be considered as stepped surfaces with an extremely high density of steps, and the step formation energy can be calculated using equation (2). In the following we shall use the notation type I and type II for the steps on $(n + 2, n + 2, n)$ and $(n + 2, n, n)$ surfaces, respectively. Figure 3 shows the structure of (331) and (211) surfaces having steps of different types. The thickness of the slabs shown there corresponds to that used in our calculations. Type I steps may have only one atomic configuration. For steps of type II, however, the position of the topmost atom (shown by the thick vertical arrow in figure 3) is not clear *a priori*. It could as easily be situated on the lattice site marked by the dashed circle corresponding to the (211) atomically flat surface. Thus we have to consider two possible atomic configurations for type II steps.
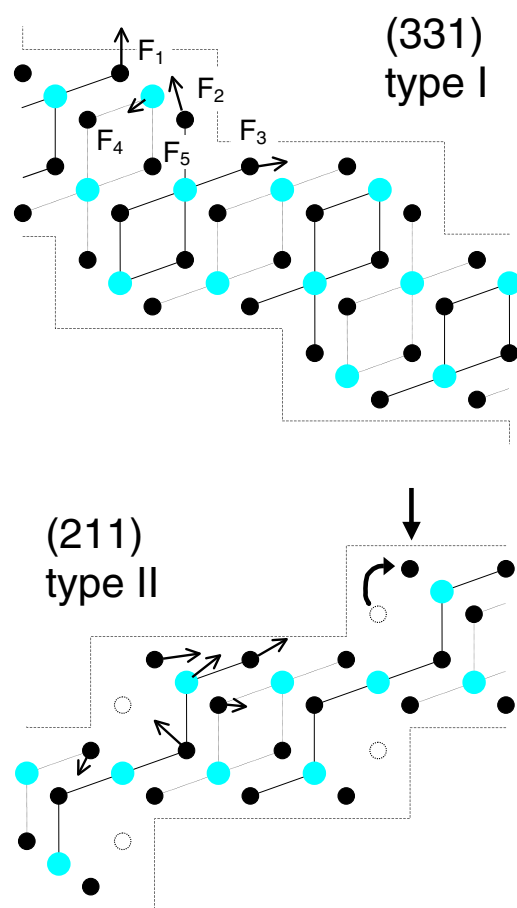

Figure 3. Cross-sections of CaF$_2$(331) and CaF$_2$(211) slabs simulating stepped surfaces in the (110) plane perpendicular to the step edge. The notation is the same as in figure 1. Steps on (331) and (211) surfaces are referred to as type I and type II steps, respectively. Dashed circles denote alternative positions of the topmost F$^-$ ion (marked by an arrow) at type II steps. Small arrows indicate the direction and relative magnitude of the displacements of atoms from their perfect-lattice sites resulting from surface relaxation. The respective displacements are listed in table 3.

Table 3. Displacements of atoms from their perfect-lattice positions at the surface of the slab corresponding to the minimum surface energy. The coordinates are chosen so that z is the direction normal to the surface plane; y is perpendicular to the step edge. Movements in the x-direction are constrained by symmetry, as well as those in the y-direction, for Ca$_1$ at the (110) 2 × 2 surface.

Slab	Atom	y (pm)	z (pm)
(331)	F$_1$	−5.7	10.3
	Ca$_1$	−5.9	−5.6
	F$_2$	−14.6	10.3
	F$_3$	8.3	−0.1
	Ca$_2$	−2.1	3.3
	F$_4$	0.6	−1.6
(211)	F$_1$	14.4	−10.6
	F$_2$	15.8	−3.1
	Ca$_1$	16.8	12.0
	F$_3$	−1.6	−2.8
	F$_4$	8.4	−0.4
	Ca$_2$	5.2	−4.7
	F$_5$	−6.2	8.5
(110) 2 × 2	F$_1$	−1.3	15.0
	Ca$_1$	—	0.9
	F$_2$	−11.3	3.7
	F$_3$	3.4	5.4
	Ca$_2$	1.6	3.3

All other possible steps with edge orientations other than [110] can be constructed from fragments of type I and type II elementary steps. These steps have no symmetry except a translation along the step edge and low-coordination F$^-$ ions at kink sites. We shall refer to such zigzag steps as type III steps. As an example of a type III step with an extremely large number of kinks, we consider a step with edges aligned along the [211] direction. The corresponding sequence of planes S_n^{III} defined by indices $(n + 4, n + 2, n)$ is also included in table 2.

Calculated surface and step energies for several CaF$_2$ surfaces are listed in table 4. As expected, the (111) surface has the lowest surface energy and the surface energy for the stepped surfaces decreases with distance between steps towards the (111) value. The step energies for type I steps are in general smaller than those for type II steps. The alternative configuration of type II steps is apparently less stable than the normal configuration. This is surprising since the alternative configuration yields a very small surface roughness and one would intuitively expect a lower surface energy for this configuration.

For selected surfaces the relaxation was determined. In contrast to the flat (111) surface, stepped surfaces have a considerable atomic relaxation. The relaxation energy is larger for less stable surfaces. Arrows in figures 3 and 4 schematically show the displacements of atoms from their lattice sites corresponding to the minimum of the total energy. The size of the arrows corresponds to the relative magnitude of displacement while absolute displacements are too small to be well represented in the figures. Numerical values of displacements are listed in table 3. The largest displacements are about 0.015 nm for both type I and type II steps.

Step energies are independent of the distance between steps when these are separated by more then 1 nm. For smaller distances a noticeable interaction between the steps is observed. For type I steps, the step energy increases with the distance between steps, while for type II it

Table 4. Surface and step energies as defined in equations (1) and (2) calculated for various regular surface structures detailed in table 2. The different types of step are described in detail in the text. The second number in each column describes properties of the relaxed surface.

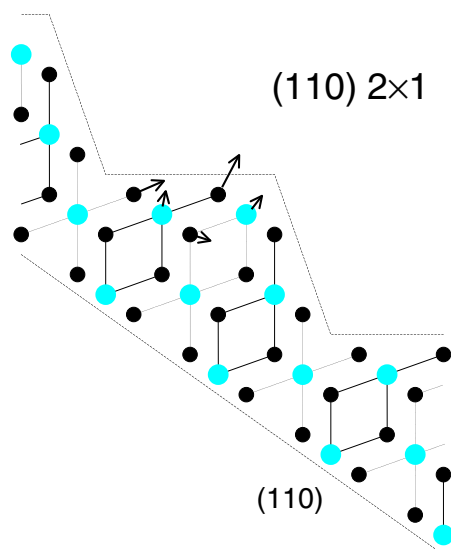|		Surface energy γ_{ijk} (J m^{-2})		Step energy ε_{st} (nJ m^{-1})	
		Non-relaxed	Relaxed	Non-relaxed	Relaxed
Perfect	(111)	0.47	0.47	—	—
Type I step	(110)	0.94	0.85	0.31	0.24
	(331)	0.81	0.72	0.32	0.25
	(221)	0.72		0.32	
Type II step	(100)	1.51	1.21	0.49	0.37
	(311)	1.14		0.47	
	(211)	0.92	0.80	0.46	0.35
Type II alternative structure	(211)	1.66	1.31	1.17	0.56
Type I double height	(110) 2 × 1	0.80	0.73	0.46	0.38
Type III step	(210)	1.43		0.54	
	(531)	1.25		0.68	

Figure 4. A cross-section of the reconstructed (110) 2 × 1 surface. The notation is the same as in figure 3.

decreases. Thus, the interaction between type I steps is attractive, but it is repulsive for type II steps. This means that the aggregation of type I steps into higher steps yields a gain in surface stability. In order to explore this tendency in more detail we calculated the structure of a (110) 2 × 1 reconstructed surface. As seen in figure 4, this surface consists of type I steps with a height corresponding to two triple layers. Such a reconstruction was found to be energetically favourable. The surface energy for the reconstructed surface is lower by 0.14 J m^{-2} than that of the normal (110) surface. We attribute this to the fact that this surface consists of facets having

the most stable (111) surface structure and we expect that the surface energy will decrease even further when increasing the width of the (111) facets. In the limiting case of large macroscopic facets, we can neglect the additional energy due to the edges and corners, and the energy of such a surface is simply given by $\gamma_{111}/\cos\alpha = 0.58$ J m^{-2}, where α is the angle between the (110) surface and (111) facets. It can also be deduced from table 4 that the formation energy of one double-height step is lower than the energy needed to form two single steps, confirming the attractive interaction between type I steps.

The type III step can be constructed from type I and type II fragments of equal length. Therefore, its energy can be estimated as a sum:

$$\varepsilon_{III} = (\varepsilon_I + \varepsilon_{II})/\sqrt{3} \tag{3}$$

where $\sqrt{3}$ accounts for the difference in length between straight and zigzag steps. This simple formula neglects the additional formation energy of kinks and corners at type III steps. Indeed the calculated step energy of 0.68 nJ m^{-1} is larger than the value of 0.45 nJ m^{-1} estimated using equation (3).

This suggests that surfaces with type III steps are likely to reconstruct in a way that reduces the number of kink sites. The precise determination of the additional energy needed to create a kink, however, would require a geometry optimization for rather complicated surfaces with large unit cells and low symmetry. Such calculations are beyond the scope of the present paper but may be subject of forthcoming work aiming to provide a detailed understanding of specific surface structures.

To demonstrate the modification of the surface electronic structure induced by steps, we present here in more detail the results of (331) surface calculations. This particular surface has the most stable steps of type I and the distance between steps is already large, so we can neglect effects of the interaction between steps on the surface energy, relaxation, and electron density of states. The total width of the F (2p) valence band at the stepped surface is larger by 0.5 eV than that of the perfect (111) surface or the bulk crystal. This is due to the split-off surface states induced by the steps above the bulk valence band maximum. The projected DOS for inequivalent F$^-$ ions at the surface of the (331) slab (see the notation in figure 3) is shown in figure 5. The enumeration follows the increasing distance of the respective atomic layer from
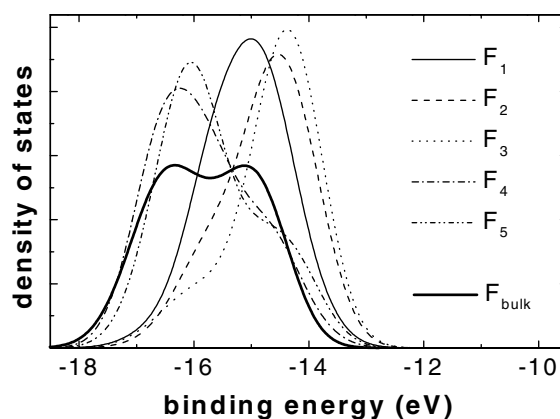

Figure 5. The density of states in the valence band projected to the F$^-$ ions at the (311) surface with steps of type I. The labels F$_i$ denote fluorine layers parallel to the (311) plane, starting from the top surface layer with F$_1$ (see the corresponding labels in figure 3). The solid bold line represents the bulk density of states.

the (331) surface plane. For comparison we have added the DOS for the bulk crystal. The bulk DOS was shifted similarly to the representation in figure 2. To determine the necessary shift, in this case we calculated the DOS in the middle of a slab containing 16 fluorine layers where the electronic properties are bulk-like. Since the Madelung potential for the (331) surface differs from that of the (111) surface, the binding energy scales of figures 2 and 5 differ by about 1 eV. The projected DOS for the F^- ions at the stepped surface (F_1, F_2, and F_3 in figure 5) have one peak shifted towards lower binding energy compared to the bulk DOS. The magnitude of the shift depends on the ion position but on average it is the same as that on the perfect (111) surface (F_1 in figure 2). The ions F_4 and F_5 exhibit a more pronounced peak at higher binding energies, similarly to F_2 at the perfect (111) surface. The projected DOS for deeper layers (not shown in the figure) has a two-peak structure similar to that of the bulk crystal.

6. Discussion and conclusions

In contrast to that at the flat (111) surface, the atomic relaxation at the stepped surfaces was found to be significant. The largest displacements of atoms from their lattice sites are those of the surface atoms (see the arrows in figures 3 and 4). Displacements are rapidly decreasing towards the middle of the slab. The general tendency in the direction of step relaxation is such that the ions situated at the step edges are moved outward from the surface, making the step 'sharper', while there are no significant inward movements. This is opposite to what is observed for steps on (100) surfaces of ionic crystals with rock-salt structure, where the relaxation yields 'smoother' steps [22] more in accordance with what one would expect intuitively. Such a surface roughening effect is especially pronounced for the (211) surface where the alternative atomic configuration with a flatter surface is less stable. The reason for this kind of instability may be the coordination numbers of surface and step ions. In the most stable configuration each F^- ion at the step edge has two nearest Ca^{2+} ions rather than the four in the bulk and only one of six nearest F^- neighbours, while in the flat configuration each surface F^- ion has three nearest F^- neighbours. Additional repulsion between these F^- ions increases the surface energy. Similarly, at the (331) surface the driving force of the atomic relaxation is the repulsion between fluorine ions from the neighbouring layers (F_2 and F_3 in figure 3).

It follows from simple geometrical considerations that steps on the (111) surface of the same type have $60°$ as the crossing angle while steps of different types cross at an angle of $120°$. This is illustrated in figure 6 where type I steps are represented by solid lines while
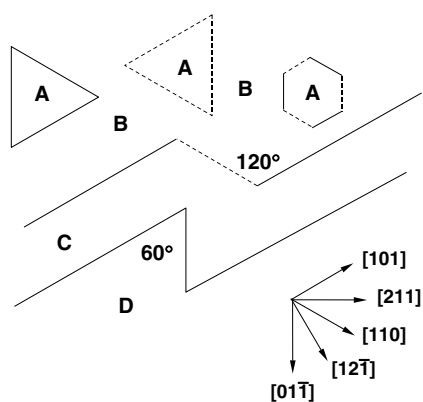

Figure 6. Possible step-crossing patterns on the $CaF_2(111)$ surface. Steps of types I and II are denoted by solid and dashed lines, respectively. The letters correspond to an increasing height of terrace: A > B > C > D.

dashed lines denote steps of type II. Since type I steps are energetically more favourable, we expect the steps on the cleaved surface to have a crossing angle of 60° rather than 120°. This correlates well with the experimental observation of a preferential formation of sharp crossing angles (less than 60°) between triple-layer steps during cleavage of CaF$_2$(111) surfaces [6, 7]. The formation of stratified rather than closed structures is fostered by the process of cleavage itself due to the preferential direction imposed by the cleavage device. Also during synthesis (i.e. the epitaxial growth of a thick CaF$_2$ film on a semiconductor substrate) in a regime where surface diffusion does not play a dominant role, protrusions with 60° edges are predominantly observed [23]. The formation energy for the type III step and for other zigzag steps of different orientation is apparently larger than that for the straight steps of type I and II due to the presence of the kink sites and corners at the step edge. Therefore, cleavage tips sharper than 60° including the 45° crossings of steps often observed experimentally cannot be explained within our static model.

None of these arguments, however, hold when additional energy is provided and distributed over the surface by heating the crystal. In this case, energy minimization is not determined by the local configuration but has to be considered on a more global scale. In this case, a closed hexagonal structure minimizing the total step length is favoured. The formation of hexagonal and trapezoidal structures by surface diffusion upon heating of CaF$_2$(111) has, in fact, been found experimentally and, in a certain temperature range, the transition from one structure to the other can be directly observed [7].

The main conclusion to be drawn from calculated surface electronic properties of stepped surfaces is that triple-layer steps do not create a significant density of states higher in the bulk band gap. The presence of steps effectively shifts the DOS of the F (2p) valence band a few hundred meV upward; this is very similar to what is calculated for the topmost layer of the perfect (111) surface. We have not performed detailed calculations for larger steps; however, one can anticipate that the findings would be similar to those for small steps since regular larger steps do not introduce new geometrical configurations that could be expected to create additional states. As a consequence, we have good reason to exclude electronic states created by steps from consideration as an origin for linear absorption of sub-band-gap laser light in CaF$_2$. For a wavelength close to half of the first excitation energy, e.g. 248 nm (5 eV) KrF excimer laser light, however, the small density of occupied states found above the bulk valence band edge might enhance two-photon absorption.

In summary, various atomic and electronic properties of CaF$_2$(111) and steps on this surface have been calculated using an *ab initio* method. We have shown that the (111) surface corresponds to almost ideal termination of the bulk crystal structure and only the topmost layer introduces a small contribution to the density of states just above the bulk valence band edge. Considerable relaxation, however, was found for various configurations of steps with one triple-layer height. According to their geometric structure, we have identified three types of step. We found that the step with the lowest formation energy is aligned along the [110] crystallographic direction. The calculated difference in formation energy for steps of different types explains the crossing angles of 60° between steps. We have also shown that steps do not introduce a considerable density of states higher in the band gap, but yield a broadening of the F (2p) valence band similar to what is calculated for the ideal surface.

References

[1] Reichling M 1998 *Laser Ablation in Optical Components and Thin Films (Experimental Methods in the Physical Sciences vol 30)* ed J C Miller and R F Haglund (San Diego, CA: Academic) p 573
Reichling M, Sils J, Johansen H and Matthias E 1999 *Appl. Phys. Suppl.* A **69** S743
[2] Mouchovski J T, Haltakov I V and Lyutskanov V L 1996 *J. Cryst. Growth* **162** 79
[3] Ando M, Negishi M, Takimoto M, Deguchi A and Nakamura N 1995 *Proc. SPIE* **2576** 348
[4] Hofmann C 1992 *Mater. Design* **13** 167
[5] *IBM J. Res. Dev.* 1997 **41** (1, 2) is a compilation of several articles about topics related to laser lithography at 193 nm.
Lerner E J 1999 *Indust. Phys.* June p 18
[6] Bennewitz R, Reichling M and Matthias E 1997 *Surf. Sci.* **387** 69
[7] Engelhardt J B, Dabringhaus H and Wandelt K 2000 *Surf. Sci.* **448** 187
[8] Gogoll S, Stenzel E, Johansen H, Reichling M and Matthias E 1996 *Nucl. Instrum. Methods* B **116** 279
[9] Huisinga M, Puchin V E and Reichling M 1998 *Nucl. Instrum. Methods* B **141** 528
[10] Stankiewicz B and Modrak P 1995 *Surf. Sci.* **331–333** 1441
[11] Jockisch A, Schroder U, de Wette F W and Kress W 1993 *J. Phys.: Condens. Matter* **5** 540
[12] Tasker P W 1980 *J. Physique Coll.* **41** C6 488
[13] Lindan P J 1995 *Phil. Mag.* **72** 601
[14] Stankiewicz B and Kisiel W 1994 *Vacuum* **45** 209
[15] Westin E, Rosén A and Matthias E 1990 *Molecular Cluster Calculations of the Electronic Structure of the (111) Surface of CaF$_2$ (Springer Series in Surface Science vol 19)* ed G Betz and P Varga (Berlin: Springer) p 316
[16] Dovesi R, Saunders V R, Roetti C, Causà M, Harrison N M, Orlando R and Aprà E 1996 *CRYSTAL95 User's Manual* University of Torino
[17] Catti M, Dovesi R, Pavese A and Saunders V R 1991 *J. Phys.: Condens. Matter* **3** 4151
[18] Ochs D, Maus-Friedrichs W, Brause M, Günster J, Kempter V, Puchin V, Shluger A and Kantorovich L 1996 *Surf. Sci.* **365** 557
[19] Hayes W 1974 *Crystals with the Fluorite Structure* (Oxford: Clarendon)
[20] Gilman J J 1960 *J. Appl. Phys.* **31** 2208
[21] Rieger D, Himpsel F J, Karlsson U O, McFeely F R, Morar J F and Yarmoff J A 1986 *Phys. Rev.* B **34** 7526
[22] Kantorovich L N, Holender J M and Gillan M J 1995 *Surf. Sci.* **343** 221
[23] Pietsch H, Klust A, Meier A and Wollschläger J 1997 *Surf. Sci.* **377–379** 909